

Superconducting transition temperatures and structure of MBE-grown Nb/Pd multilayers

S. Kaneko,* U. Hiller, J. M. Slaughter,† and Charles M. Falco

Department of Physics and Arizona Research Laboratories, University of Arizona, Tucson, Arizona 85721

C. Coccorese and L. Maritato

Dipartimento di Fisica, Università degli Studi di Salerno, Baronissi (Sa), I-84081, Italy

(Received 10 July 1997)

We have studied the structure and superconducting properties of molecular-beam-epitaxy-grown Nb/Pd multilayers. The resistivity of each layer was calculated from the multilayer resistivity by including size effect and bulk imperfection terms. The superconducting transition temperatures obtained using these resistivities together with the de Gennes–Werthamer theory showed good agreement with the experimental results. [S0163-1829(98)05737-3]

I. INTRODUCTION

The coexistence of superconductivity and magnetism has been observed previously, when it was shown that ferromagnetism and antiferromagnetism coexist with superconductivity in molybdenum chalcogenides¹ and rhodium boride² compounds. Other more recent studies show that superconductivity also can coexist with spin glasses.^{3–6} Because of the multiple magnetic phases that occur in relatively dilute Pd-Mn alloys,^{7,8} we are interested in the superconducting properties of Nb/Pd_{1-x}Mn_x multilayers, beginning with Nb/Pd.

The theory that describes the proximity effect between a normal metal and superconductor was proposed by de Gennes,⁹ and extended to magnetic materials by Werthamer.¹⁰ However, for the de Gennes–Werthamer (dGW) theory to apply, the electron mean free path (mfp) must be smaller than the layer thickness, $d_i > \ell_i$. The resistivity of each layer is required to determine the mfp. For sputtered samples, measurements of thick film resistivity at low temperature are often used to obtain the mfp. However our thick films prepared by molecular-beam epitaxy (MBE), had large mean free paths that are not representative of the mfp in the layers of our multilayers. Therefore we used the multilayer resistivity data to determine the mfp in each layer by assuming resistivity is caused by a size effect,^{11–13} along with imperfections including impurities, grain size, and other contributions.

II. EXPERIMENTAL PROCEDURES

Multilayer samples were prepared in a Perkin-Elmer 433S MBE system with a base pressure of $\sim 5 \times 10^{-11}$ Torr. 4° miscut Si(111) substrates were used to grow Nb/Pd multilayers on 40-Å Cu buffer layers. The Si(111) substrates were first dipped in a 2% HF acid solution for 2 min and then immediately loaded into the ultrahigh vacuum (UHV) chamber via a load lock. The substrates next were annealed in UHV at 750° for 15 min in order to drive off hydrocarbons, and reflection high-energy electron diffraction (RHEED) and low-energy electron diffraction (LEED) employed to verify the 7×7 reconstruction of the Si. After the substrate cooled

to room temperature, a 40-Å Cu layer was deposited by *e*-beam evaporation as a buffer layer for the subsequent growth. Although there is a 15% lattice mismatch, the 40-Å Cu layer grows epitaxially on Si(111) by forming an intermediate silicide.^{14–16} We also verified the Cu(111) plane was rotated 30° with respect to the Si(111) surface. The deposition rates for Cu, Nb, and Pd were 0.4, 0.1, and 0.2 Å/s, respectively. Five bilayers of Nb(110)/Pd(111) were deposited on the buffer layer, and we verified epitaxial growth of each multilayer with RHEED and LEED. Having five bilayers minimizes the effects of the underlayer and top layer oxidation on the superconducting properties, as well as making detailed x-ray analysis possible. A moving shutter was used to produce regions with different Pd thickness across the three-inch wafers.

We used x-ray diffraction (XRD) and low-angle x-ray reflectivity (XRR) to determine the thickness of each layer and to verify the crystal structure. The resistivities of the multilayers were measured by the van der Pauw method, down to 4.2 K.

III. RESULTS AND DISCUSSION

The RHEED and LEED patterns are indicative of epitaxial layers with limited in-plane order. As shown in Fig. 1, the RHEED patterns consist of bulbous, somewhat diffuse streaks typical of a surface that is not atomically flat and somewhat disordered, although still having a well-defined

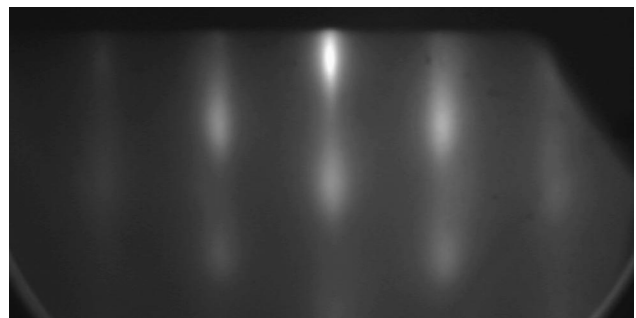


FIG. 1. A typical RHEED pattern of the surface of a Nb layer along the $[1\bar{1}\bar{1}]$ direction.

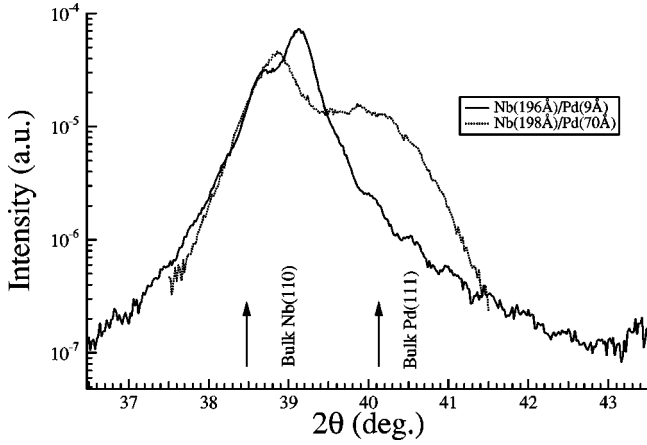


FIG. 2. XRD spectra of two Nb/Pd multilayers with five bilayers each, thicknesses as indicated. The thin-Pd sample exhibits superlattice satellite peaks.

orientation. The short in-plane coherence is likely due to a relatively high density of grain boundaries needed to relieve the stress caused by the symmetry difference between the fcc-Pd (111) and bcc-Nb (110) planes. Interestingly, the XRD spectra exhibit superlattice peaks which demonstrate that the crystalline coherence in the perpendicular direction extends over several periods, i.e., many hundreds of Angstroms. Figure 2 shows the $\theta-2\theta$ XRD for samples with the thickest, 80 Å, and thinnest, 10 Å, Pd layers. The thin-Pd sample exhibits clear superlattice satellites while the thick-Pd XRD looks more like separate Nb and Pd peaks. The thick-Pd result is typical for multilayers with such a large period. The rocking curve widths for these peaks are 2–2.5 deg full width at half maximum. This spread of crystallite orientations is much narrower than typical sputter-deposited multilayers but not as narrow as the highest quality metallic superlattices. The XRR shows that the layers are well-defined with rms interface roughnesses on the order of 10 Å. Taken together, these measurements show that the structure is an epitaxial mosaic with columns that are very long in the (111)/(110) direction but relatively small in diameter. Although the interface roughness corresponds to several atomic spacings, it is much smaller than the superconducting coherence length which is several hundred Angstroms. The layer thicknesses obtained by fitting the XRR spectra is included in Table I.

TABLE I. Summary of Nb/Pd multilayered samples. ρ_m is the resistivity of the multilayer. All the samples were deposited on 4° miscut Si(111) substrate.

Sample	Measurement (Nb/Pd) (Å)	period Λ (Å)	ρ_m ($\mu\Omega$ cm)	T_c (K)
1a	196/9	205	8.10	8.70
1b	195/18	213	8.05	8.10
1c	196/25	221	8.03	7.85
1d	196/31	227	8.02	7.10
2a	198/21	219	8.18	8.02
2b	198/42	240	8.15	7.55
2c	198/58	256	8.00	7.40
2d	198/70	268	7.85	7.24

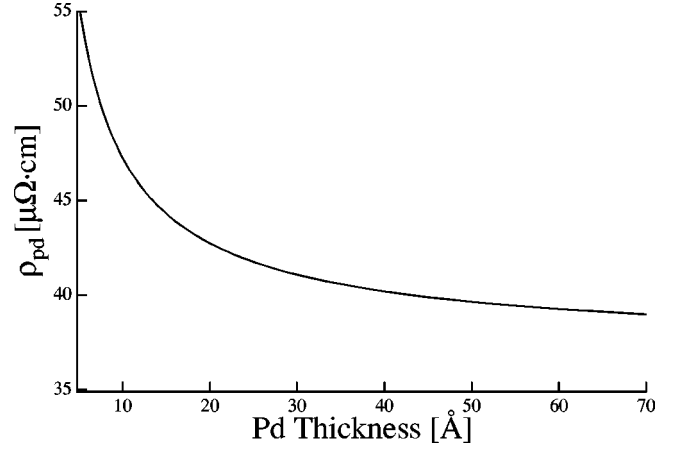


FIG. 3. Pd resistivity in a multilayer, calculated from the multilayer resistivity at low temperature (10 K).

To apply the de Gennes–Werthamer theory to the Nb/Pd multilayers, the resistivity of each layer in the multilayer is required. To determine the resistivity, we assumed a parallel resistor model for the multilayer structure, so that

$$\frac{1}{\rho_m} = \frac{1}{\rho_{Nb}} + \frac{1}{\rho_{Pd}}, \quad (3.1)$$

where ρ_m , ρ_s , and ρ_n are the resistivity of a multilayer, superconductor (Nb) and normal metal (Pd), respectively. This model is valid when interface scattering is completely diffuse, and is a good approximation when the mfp's are limited by substantial interfacial on other scattering as indicated by the resistivity measurements of these samples. Since the thickness of the Nb layer is a constant ~ 200 Å, we assume the resistivity of each Nb layer is constant. Assuming the resistivity of the Pd layers is limited by the size effect^{17–19} and imperfections in the layers, the resistivity can be expressed by

$$\rho_{Pd} = \rho_{Pd}^{\text{bulk}} + \rho_{Pd}^{\text{SE}} + \rho_{Pd}^i, \quad (3.2)$$

where the contributions ρ_{Pd}^{bulk} , ρ_{Pd}^{SE} , and ρ_{Pd}^i are due to the bulk, size effect, and imperfections including impurities, not found in the “bulk” thick-film material. The size effect ρ_{Pd}^{SE} has the form

$$\rho_{Pd}^{\text{SE}} = \frac{4}{3} \frac{1}{\gamma(1+2p)} \frac{1}{\ln(1/\gamma)}, \quad (3.3)$$

where γ is the ratio of the film thickness to the mean free path, d_{Pd}/ℓ_{Pd} , and p is a fraction of the electrons scattered elastically from both surfaces of the film (specular scattering). Note that, for our MBE-grown Pd, ρ_{Pd}^{bulk} is negligible compared to other terms.

The resistivities of the Nb and Pd layers were obtained by fitting the resistivity data using Eqs. (3.1) and (3.3) as a function of the Pd thickness. For the size effect, we assumed the complete diffuse scattering case ($p=0$) in Eq. (3.3). We estimate the resistivity of Nb to be ~ 10 $\mu\Omega$ cm, and that of the Pd layers we calculate to be 40–50 $\mu\Omega$ cm, as shown in Fig. 3. These resistivities for the Pd layers are comparable to the recent experimental results of Hloch and Wissmann.²⁰ For the Nb layers, the resistivities were the same as for our

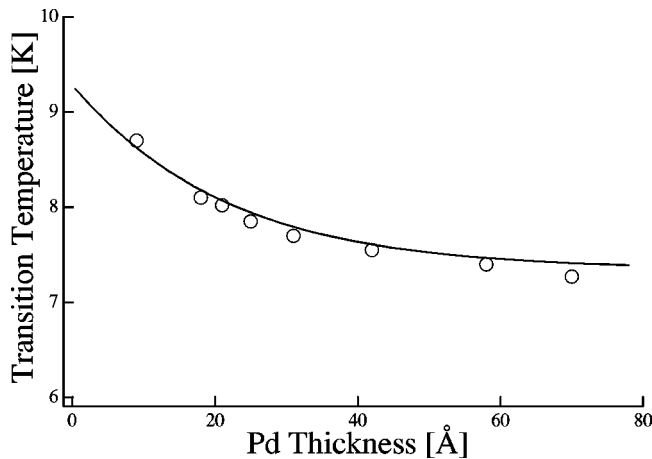


FIG. 4. Transition temperature of Nb/Pd multilayers with a 200 Å Nb layer thickness. The solid line is calculated using de Gennes–Werthamer theory with no adjustable parameters.

previous samples.²¹ From the resistivities, the mfp of each layer was calculated to be 35 Å for the Nb layer, and 8–10 Å for the Pd layers. Using these values, T_c of the multilayers can be calculated from the de Gennes–Werthamer theory.

The equations of de Gennes–Werthamer^{9,10} theory were used to calculate the transition temperatures, T_c , with the well-known expression²²

$$\frac{k_n}{\rho_n} \tanh(k_n d_n) = \frac{k_s}{\rho_s} \tan(k_s d_s), \quad (3.4)$$

where ρ is the resistivity, k is the wave vectors and d is the layer thicknesses. The indices n and s stand for normal metal and superconductor, respectively.

In Ref. 22, the author mentioned that the equations for multilayer sample may be the same as the single bilayer and showed that a three-bilayer sample had the same T_c as the single bilayer. We applied the single bilayer equation to our five-bilayer samples. Figure 4 shows the experimental data and the calculated T_c as a function of the Pd thickness. As can be seen, the solid line in Fig. 4 describes the experimental data with good agreement.

In summary, we have grown epitaxial, coherent Nb/Pd multilayers by MBE and have shown that their transition temperatures are in good agreement with the de Gennes–Werthamer theory. It is important to use layer resistivities extracted from the multilayer data rather than thick-film values or even size-effect-corrected values when doing the dGW calculation. Layer resistivities are higher than expected by including a size-effect correction to the thick-film values. The additional increase in resistivity in the layers is probably due to stress-induced dislocations in this bcc/fcc system.

ACKNOWLEDGMENTS

We wish to acknowledge J. T. Eickmann for useful suggestions and support. This research was supported in part by the U.S. Office of Naval Research under Contract No. N0014-92-J-1159.

*Current address: Industrial Research Institute, Kanagawa Prefecture Government, 705-1 Shimo-Imaizumi, Ebina, Kanagawa 243-04 Japan.

†Current address: Motorola, Phoenix Corporate Research Laboratories, EL308, 2100E Elliot Rd., Tempe, AZ 85284.

¹M. Ishikawa and Ø. Fisher, *Solid State Commun.* **23**, 37 (1977).

²W. A. Fertig, D. C. Johnston, L. E. DeLong, R. W. McCallum, M. B. Maple, and B. T. Matthias, *Phys. Rev. Lett.* **38**, 987 (1977).

³D. Hüser, M. J. F. M. Rewiersma, J. A. Mydosh, and G.J. Nieuwenhuys, *Phys. Rev. Lett.* **51**, 1290 (1983).

⁴M. Mauere, A. Menny, M. F. Ravet, J. Meiresonne, P. H. Kes, and J. A. Mydosh, *Phys. Rev. B* **40**, 5198 (1989).

⁵M. L. Wilson, R. Loloee, and J. A. Cowen, *Physica B* **165-166**, 457 (1990).

⁶C. Attanasio, L. Maritato, S. L. Prischepa, M. Salvato, B. N. Engel, and C. M. Falco, *J. Appl. Phys.* **77**, 2081 (1995).

⁷W. M. Star, S. Foner, and E. J. McNiff, Jr., *Phys. Rev. B* **12**, 2690 (1975).

⁸G. Williams, *Magnetic Susceptibility of Superconductors and*

Other Spin Systems (Plenum, New York, 1992), p. 475.

⁹P. G. de Gennes and E. Guyon, *Phys. Lett.* **3**, 168 (1963).

¹⁰N. R. Werthamer, *Phys. Rev.* **132**, 2440 (1963).

¹¹J. J. Thomson, *Proc. Cambridge Philos. Soc.* **11**, 120 (1901).

¹²K. Fuchs, *Proc. Cambridge Philos. Soc.* **34**, 100 (1938).

¹³F. H. Sondheimer, *Phys. Rev.* **80**, 401 (1950).

¹⁴F. J. Walker, E. D. Specht, and R. A. McKee, *Phys. Rev. Lett.* **67**, 2818 (1991).

¹⁵Chin-An Chang, *J. Appl. Phys.* **67**, 566 (1990).

¹⁶C. S. Liu, S. R. Chen, W. J. Chen, and L. J. Chen, *Mater. Chem. Phys.* **36**, 170 (1993).

¹⁷J. J. Thomson, *Proc. Cambridge Philos. Soc.* **11**, 120 (1901).

¹⁸K. Fuchs, *Proc. Cambridge Philos. Soc.* **34**, 100 (1938).

¹⁹F. H. Sondheimer, *Phys. Rev.* **80**, 401 (1950).

²⁰H. Hloch and P. Wissmann, *Phys. Status Solidi A* **145**, 521 (1994).

²¹C. W. Wilks, B. N. Engel, and C. M. Falco, *J. Appl. Phys.* **76**, 6959 (1994).

²²P. R. Broussard, *Phys. Rev. B* **43**, 2783 (1991).